ROYAL SOCIETY
OF CHEMISTRY

EDGE ARTICLE

Check for updates

All publication charges for this article
have been paid for by the Royal Society
of Chemistry

A color-tunable single-component luminescent molecule with multiple emission centers†

Junru Chen,[a] Xiaojie Chen,[b] Yanyan Liu,[b] Yang Li,[c] Juan Zhao, *[a] Zhiyong Yang,[b]
Yi Zhang *[b] and Zhenguo Chi *[ab]

For achieving smart materials with color-tunable emissions, the development of single-component systems exhibiting high durability and stability is desired but remains challenging, in comparison to multicomponent systems. Here, a single-component luminescent molecule (3-SPhF) with colorful emissions is successfully reported through different expressions of triplet excitons in radiative transitions. The time-resolved spectra confirm the existence of delayed fluorescence ($\tau = 282.5$ µs), monomeric phosphorescence ($\tau = 497.7$ ms) and aggregated-state phosphorescence ($\tau = 230.0$ ms) in the crystal powder of 3-SPhF, which affords time-dependent afterglow and excitation-dependent emissions in a steady state. Furthermore, the relationships between ultra-long luminescence and stacking of the dibenzofuran group in single crystals are explored, providing evidence for the regularity of multiple emission centers in single-component compounds with dibenzofuran substituents.

Introduction

Stimuli-responsive luminescent materials are usually accompanied by variable emission colors, showing promising applications in anti-counterfeiting, information encryption and biological engineering.[1-8] Luminous colors regulated by physical stimulation endow smart materials with abundant optical properties. To obtain multicolor emissions, the focus of previous reports mainly relied on multicomponent luminescence for example from a mixture of chromophores, multicomponent dimers and trimers, and terpolymers.[9,10] In spite of that, ideal systems are multicolor single crystals because of their excellent durability and stability. Unfortunately, the majority of single-component materials only tend to interconvert between colored and colorless.[11-13] Although a few modulations, including isomers and crystallinity,[14-16] have succeeded in achieving multicolor emissions, developing high efficiency single-component materials with tunable emission colors is a great challenge.

As is well known, luminescence involving triplet excitons can be expressed in many forms. Inspired by multiple emission centers in carbon dots, An *et al.* realized tunable persistent luminescence under different excitations through constructing multiple ultra-long organic phosphorescence emitting centers in a single-component molecular crystal.[17] Except for phosphors, delayed fluorescence had also been used in developing dynamically controlled afterglow.[18,19] Therefore, the different expressions of triplet excitons provide a high possibility to achieve colorful emissions in single-component materials.[20,21] However, strategies based on triplet exciton controlling to tune emission colors are still rare and short of regularity.

In our previous work, time-dependent afterglow was firstly discovered in a dibenzofuran-containing single-component molecule with room temperature phosphorescence (RTP) and delayed fluorescence (DF).[22] It was speculated that intermolecular hydrogen-bonding interactions are beneficial for DF enhancement, and meanwhile it is important to rationally construct multiple emission centers for achieving color-tunable single-component compounds. Nevertheless, there is still considerable ambiguity with regard to the derivation of DF with ultra-long lifetimes and high efficiency. Therefore, in order to explore the origin and regularity of DF, in this work, dibenzofuran-containing compounds are designed and investigated, on the basis of photophysical property studies of our previous dibenzofuran chromophores. The dibenzofuran compound was also synthesized[23] by us in this work and the purity analyses were carried out using nuclear magnetic resonance (NMR) and high-resolution mass spectra (HRMS) (Fig. S1–S3†). Unexpectedly, the photoluminescence (PL) spectrum of the dibenzofuran crystal shows dual emission peaks at

aSchool of Materials Science and Engineering, Sun Yat-sen University, Guangzhou 510275, China. E-mail: zhaoj95@mail.sysu.edu.cn

bPCFM Lab, GDHPPC Lab, Guangdong Engineering Technology Research Center for High-performance Organic and Polymer Photoelectric Functional Films, State Key Laboratory of OEMT, School of Chemistry, Sun Yat-sen University, Guangzhou 510275, China. E-mail: ceszy@mail.sysu.edu.cn; chizhg@mail.sysu.edu.cn

cInstrumental Analysis and Research Center (IARC), Sun Yat-sen University, Guangzhou 510275, China
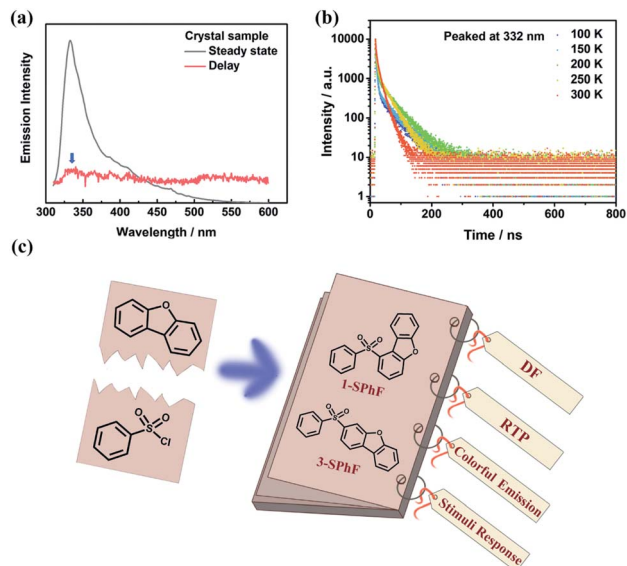
Fig. 1 (a) The PL spectra of dibenzofuran in a crystalline state; (b) temperature-dependent emission decay spectra at 332 nm for dibenzofuran; (c) the structure and properties of 1-SPhF and 3-SPhF.

332 nm and 410 nm in a steady state (Fig. 1a). According to temperature-dependent emission decay spectra (Fig. 1b and S11†), the corresponding lifetime of the peak at 410 nm decreases as the temperature increases from 100 K to 300 K, contributing to RTP (Fig. S11†). However, the lifetime of emission at 332 nm could be fitted by two exponential functions below 200 K and it increases when the temperature increases from 100 K to 200 K, indicating that the triplet excitons are activated in this process.[24] Therefore, the violet emission includes traditional fluorescence and delayed fluorescence (Fig. 1b). Notably, dibenzofuran shows a very low component of DF, which is almost overlapped with conventional fluorescence, thus affecting the tendency of fluorescence at different temperatures. As a result, the lifetime of emission peaked at 332 nm displays an opposite tendency around 200 K. In addition, the component of DF is too low to be observed in the

phosphorescence spectrum after removing the UV lamp, and the almost overlapped fluorescence and DF make it difficult to verify the origin of DF from the concentration-dependent emission spectra of dibenzofuran (ca. 332 nm, Fig. S12†). In light of this, we design two isomeric molecules namely 1-SPhF and 3-SPhF (Fig. 1c), which are based on the one step reaction of benzenesulfonyl chloride and dibenzofuran. On the one hand, these compounds without extra groups are beneficial for us to further investigate the relationship between DF and stacking of neighboring dibenzofuran groups. On the other hand, the target compounds involve two different excited-state configurations ($n\pi^*$ and $\pi\pi^*$) that facilitate the production of RTP.[25,26] In this case, our groups attempt to achieve the derivatives of dibenzofuran with multiple emission centers to realize colorful emission for single component molecules.

Results and discussion

The purity of 1-SPhF and 3-SPhF was confirmed by NMR, and high-resolution EI mass (Fig. S4–S9†). Single crystals of the two isomers are obtained from slow evaporation of tetrahydrofuran/n-hexane solutions at room temperature. Moreover, the powder X-ray diffraction of 1-SPhF and 3-SPhF was conducted as shown in Fig. S10.† The CCDC numbers of 1-SPhF and 3-SPhF are 2057821 and 2057825, respectively.

For isolated molecules in dilute tetrahydrofuran solution (1 × 10⁻⁵ mol L⁻¹), the UV-vis absorption and PL spectra (Fig. S13†) of 1-SPhF exhibit a bathochromic shift in comparison to those of 3-SPhF because of steric hindrance. Similar to dibenzofuran, the crystal powders of 1-SPhF and 3-SPhF show multi-emission afterglow after removing the UV excitation (λ_{ex} = 365 nm, Fig. 2a). Particularly for 3-SPhF, three emission centers can be clearly distinguished from the emission decays (Fig. 2b). The peaks at 423 nm, 510 nm and 586 nm are observed successively during the delay time from 8 ms to 440 ms, implying the existence of tri-emission afterglow in the 3-SPhF crystal. In contrast, as the delay time changes, no extra emission peaks appear for 1-SPhF with two peaks maintained at 403 nm and 563 nm (Fig. S14†).
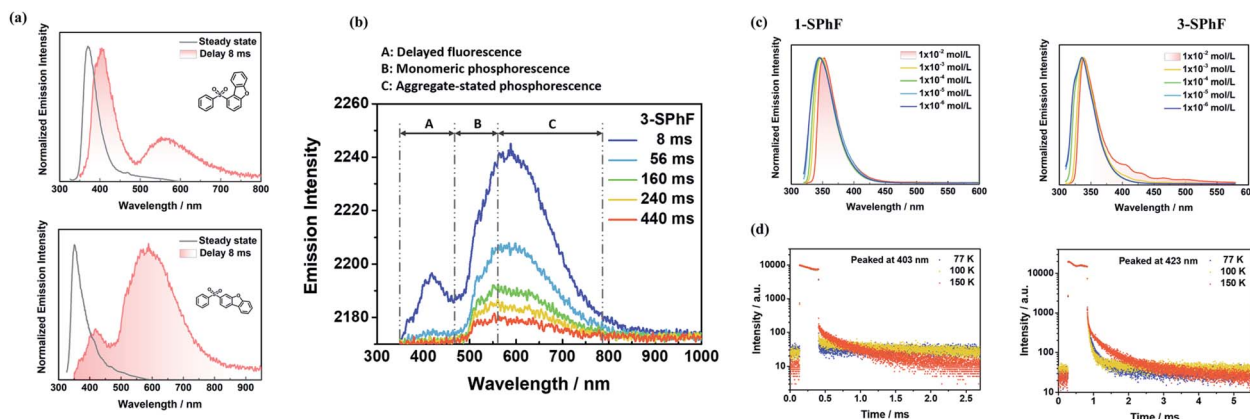

Fig. 2 (a) PL spectra of 1-SPhF and 3-SPhF in a crystalline state; (b) time-resolved phosphorescence spectra of 3-SPhF; (c) concentration-dependent spectra in toluene and (d) temperature-dependent emission decay spectra of 1-SPhF and 3-SPhF.
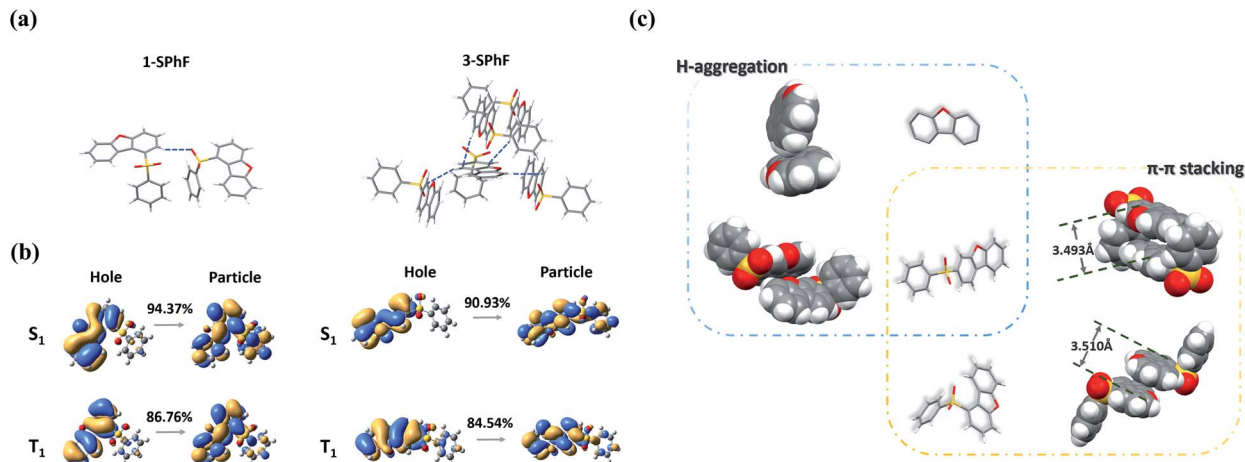
Edge Article

Fig. 3 (a) The intermolecular interaction in single crystals of 1-SPhF and 3-SPhF; (b) NTO analysis of 1-SPhF and 3-SPhF; (c) molecular packing in single crystals of dibenzofuran, 1-SPhF and 3-SPhF.

To further confirm the origin of afterglow, concentration-dependent PL spectra were measured in toluene (TOL) solutions (Fig. 2c and S15†). As the concentration increases from 1 × 10^{-6} mol L^{-1} to 1 × 10^{-2} mol L^{-1}, the peak around at 423 nm is observed in 3-SPhF rather than in 1-SPhF with hardly changed peaks. As displayed in Fig. S16,† the PL spectrum of 1-SPhF in an amorphous state only exhibits faint phosphorescence, revealing that its higher energy emissions only exist in the crystal state. The results suggest that the peaks at 403 nm (for 1-SPhF) and 423 nm (for 3-SPhF) are related to intermolecular interactions. Furthermore, the phosphorescence spectra of isomeric molecules and dibenzofuran in dilute 2-methylte-trahydrofuran at 77 K were investigated (Fig. S17†). Their similar emissions peaked at 500 nm indicating that the emission center of monomeric phosphorescence stems from dibenzofuran. Moreover, as seen from Fig. 2d, the temperature-dependent emission decay spectra of these two compounds recorded at 403 nm and 423 nm demonstrate obvious delayed fluorescence components owing to the thermal activation of triplet excitons by increasing the temperature. The gradually enhanced intensity of emissions peaked at 403 nm and 423 nm at higher temperatures and in vacuum further verify the existence of DF in 1-SPhF and 3-SPhF (Fig. S18 and S19†). In contrast, the lifetime of emissions at 563 nm (for 1-SPhF) and 586 nm (for 3-SPhF) increases sharply as the temperature decreases from 300 K to 100 K, attributed to RTP with electronic coupling for isomeric molecules (Fig. S20 and S21†).[25] Therefore, multiple emission centers are realized in both 1-SPhF and 3-SPhF by combining intermolecular DF and persistent RTP.

To further investigate the mechanism of multiple emission centers for isomeric molecules, single-crystal X-ray diffraction measurements were carried out. The results show that both 1-SPhF and 3-SPhF exhibit interactions between oxygen and hydrogen from the neighboring sulfonyl group (C–H⋯O) (Fig. S22†). Nevertheless, the dibenzofuran group in 3-SPhF is restricted by four neighboring molecules through C–H⋯π interactions, while only one interaction between sulfonyl and dibenzofuran (C–H⋯O) is observed in 1-SPhF, as displayed in Fig. 3a. Given the fact that the emission center of monomeric phosphorescence for the two compounds originates from the dibenzofuran group, 3-SPhF with four surrounding molecules demonstrates outstanding monomeric phosphorescence properties due to the limitation of non-radiative transition.

The achievement of visible DF provides a higher possibility to design color tunable luminescent materials. To date, there is still a high demand for a deeper understanding of the origin mechanism of DF, which is likely conceivable based on the exploration of the presented two isomeric molecules. Due to concentration-dependence of DF and the large energy differences between the lowest singlet (S_1) and the lowest triplet (T_1) states for monomeric 1-SPhF (ΔE_{ST} = 0.71 eV) and 3-SPhF (ΔE_{ST} = 0.83 eV) (Fig. S23†), two neighboring molecules in the single crystals are modelled for theoretical calculations. The ΔE_{ST} values were found to range from 0.60 eV to 1.09 eV, which are
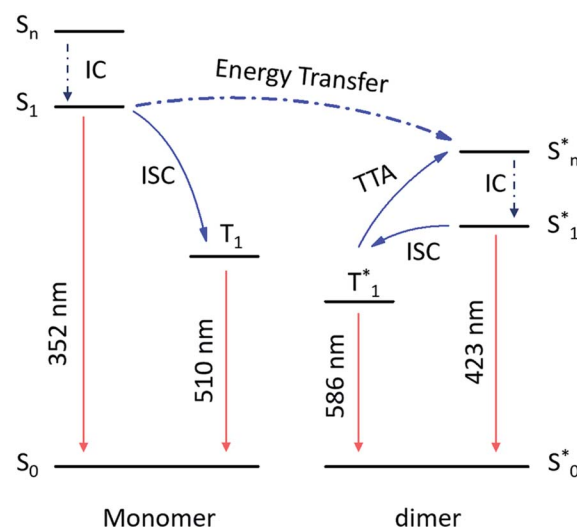

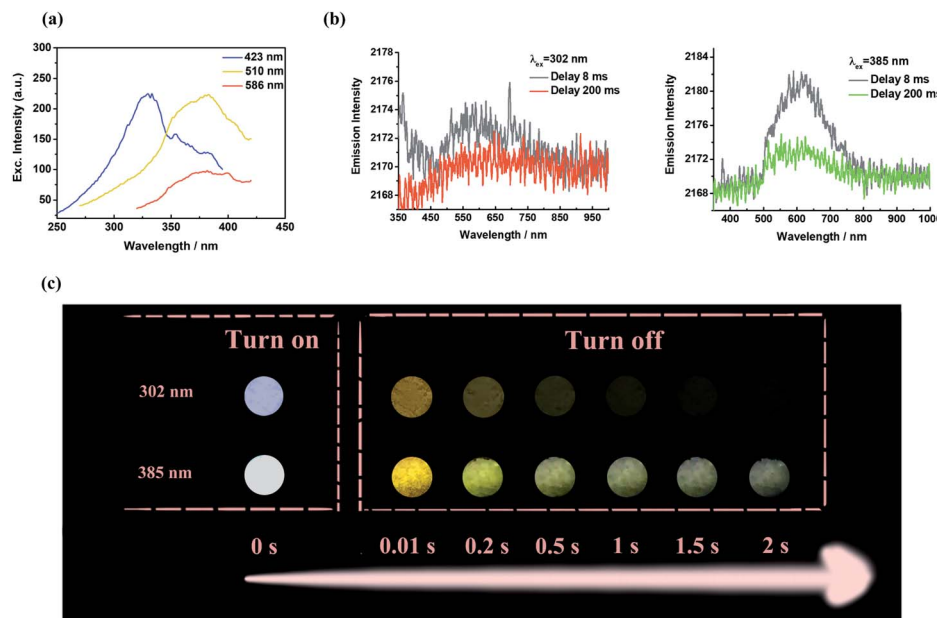**Fig. 4** The mechanism of multiple emission centers for 3-SPhF.

Fig. 5 (a) The excitation spectra of 3-SPhF at different excitation wavelengths; (b) phosphorescence spectra and (c) photographs of 3-SPhF under 302 nm and 385 nm excitations.

too large to trigger reverse intersystem crossing (rISC) for enabling thermally activated delayed fluorescence (TADF) in these coupled molecules (Table S1†). Therefore, the recognized DF of dibenzofuran-containing compounds is assigned to triplet–triplet annihilation (TTA). The bimolecular TTA process occurs when two of accumulated triplet excitons migrate and interact with each other before they are deactivated. Moreover, the occurrence of TTA is dependent on the overlapping of π-orbitals in adjacent molecules.[27,28] As aforementioned, the similar phosphorescence spectra of dibenzofuran, 1-SPhF and 3-SPhF in dilute solution at 77 K verify that the monomeric phosphorescence stems from the dibenzofuran group. Besides, nature transition orbitals (NTO) analysis[29] reveals that the T_1 of two isomeric molecules are mainly contributed by the dibenzofuran group (Fig. 3b). Therefore, the arrangement of dibenzofuran groups in the single crystals is related to the occurrence of TTA. The molecular packing in single crystals of dibenzofuran, 1-SPhF and 3-SPhF is displayed in Fig. 3c and S22.† The common π···π stacking of dibenzofuran groups is observed in 1-SPhF (3.510 Å) and 3-SPhF (3.493 Å) and provides a large orbital overlap of adjacent molecules in their single crystals, contributing to efficient TTA emissions. However, the dibenzofuran molecule only presents H-aggregation in single crystals with negligible T_1 orbital overlap, leading to weak DF.

From the above discussion, the proposed mechanism of multiple emission centers for 3-SPhF could be summarized in Fig. 4. Following UV excitation, monomeric molecular fluorescence (352 nm) and phosphorescence (510 nm) are generated through the internal conversion (IC) process from the singlet excited state (S_n) to S_1 and intersystem crossing (ISC) from S_1 to T_1, respectively. According to the concentration-dependent spectra of 3-SPhF (Fig. 2c and S15†), delayed fluorescence from 423 nm gradually increases accompanied by decreasing of

monomeric fluorescence when the concentration increases from 1×10^{-6} mol L^{-1} to 1×10^{-2} mol L^{-1}. This means that energy transfer occurs from monomeric molecular S_1 to aggregated-state S_n*. The phosphorescence of 586 nm belongs to the aggregated-state phosphorescence from T_1*, while an encounter between two triplet excitons leads to the TTA emission (423 nm).

In comparison to 1-SPhF, 3-SPhF with tri-emission afterglow exhibits more excellent properties (Table S1†), including longer lifetimes ($\tau_{423\ nm} = 282.5$ μs, $\tau_{510\ nm} = 497.7$ ms, $\tau_{586\ nm} = 230.0$ ms) and a higher efficiency ($\Phi_{DF+RTP} = 26\%$). These characteristics are responsible for the dynamic visible afterglow observed in 3-SPhF during different decay times (Fig. 5c). As mentioned above, the radiative transitions of triplet excitons in 3-SPhF are expressed through DF, monomeric phosphorescence and aggregated-state phosphorescence. The excitation spectra in Fig. 5a reveal the differences of the maximum excitation wavelength considering the three emission bands. Delayed fluorescence peaking at 423 nm can be effectively excited by UV excitation ranging from 250 nm to 350 nm, and the overlapped excitation wavelengths from 350 nm to 410 nm prefer to excite RTP. However, the orange emission is always more intense than the blue emission although the luminescence is dominated by DF at an excitation wavelength of 302 nm, owing to rapid decay of DF (Fig. 5b). Thereby, it is difficult for 3-SPhF to achieve excitation-dependent afterglow. On the other hand, when the 3-SPhF powder is excited by 385 nm UV light, the color of afterglow changes from orange to green during the delay time from 0.01 s to 2 s (Fig. 5c). This behavior of time-dependent afterglow is hardly observed in 1-SPhF but is observed in 3-SPhF, given the two ultra-long phosphorescence in 3-SPhF and a slower emission decay of its monomeric phosphorescence (Fig. 5b and Table S1†). Therefore, by varying the emission decay time, the
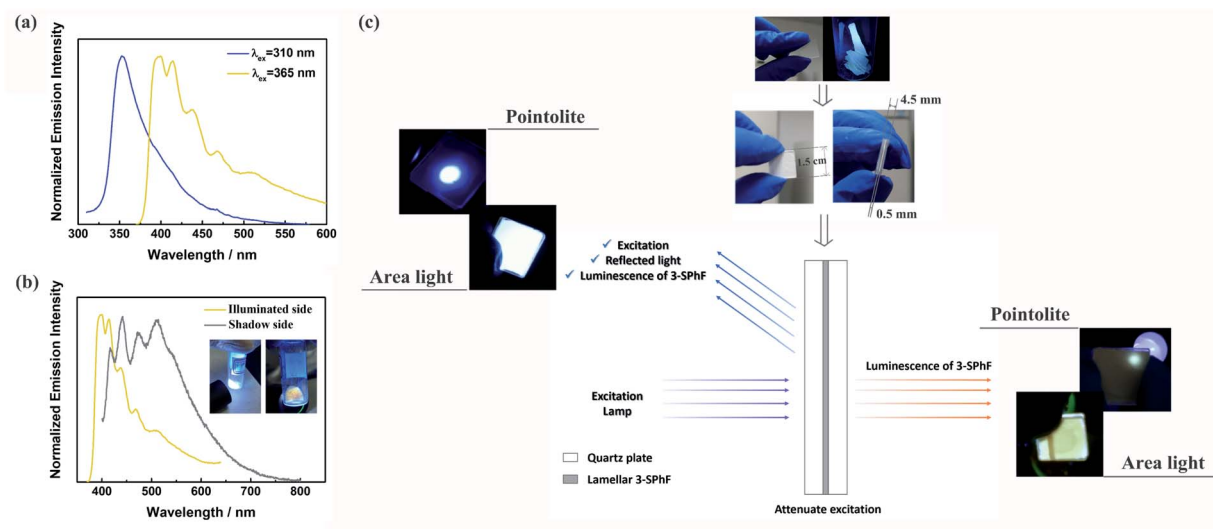
Fig. 6 (a) Normalized steady-state PL spectra of 3-SPhF at different excitation wavelengths; (b) PL spectra of illuminated and shadow sides for the 3-SPhF crystal powder (λ_{ex} = 365 nm); (c) photographs and mechanism for different color emissions of lamellar compounds at illuminated and shadow sides.

proportion of multiple emissions can be regulated, leading to dynamic time-dependent colorful afterglow for 3-SPhF.

Although excitation-dependent afterglow is difficult to realize for 3-SPhF owing to the rapid decay of DF at 423 nm, the high efficiency of DF leads to possibility of achieving colorful emission in a steady state by changing the excitation wavelength. In order to prove this hypothesis, the excitation-dependent spectra in a steady state were measured (Fig. 6a). When excited by a 310 nm UV lamp, the fluorescence emission shows a peak at 352 nm, which disappears in the PL spectrum with an excitation wavelength of 365 nm, resulting in obvious emissions of DF and RTP. However, the emission color (cold white) observed by the naked eye from the illuminated side of the 3-SPhF powder cannot be reflected from the corresponding spectrum (dominated in blue region) recorded under 365 nm UV light, while the shadow side of the 3-SPhF powder exhibits yellow emission (Fig. 6b). Furthermore, the PL spectrum of the illuminated side of the 3-SPhF powder is similar to that of the shadow side when the compound is excited by a 365 nm UV light, despite the different intensities of the emission peaks. In contrast, as for 1-SPhF, the emission color has no changes in any cases due to extensive overlap between fluorescence and DF (Fig. S24†). This phenomenon is speculated due to the fact that the excitation source and other reflected lights are difficult to be ignored by the naked eye. Using the 3-SPhF powder to attenuate the intensity of excitation, the intrinsic emission color of the compound can be extracted (Fig. 6c). Importantly, to get a more intuitive view of the difference in luminescence colors between the illuminated side and shadow side of the 3-SPhF powder, we put the lamellar compound achieved through recrystallization and extraction filtration into a quartz plate (Fig. 6c).The square area of the quartz plate is 1.5 cm × 1.5 cm, and the width of the lamellar compound is about 0.5 mm. The illuminated side of the square displays violet emission while the shadow side presents yellow emission (Fig. 6c and video S1†), attributed to

intrinsic luminescence of 3-SPhF with DF and RTP features, respectively.

Conclusions

In this work, two isomeric molecules 1-SPhF and 3-SPhF were designed by using dibenzofuran as a chromophore, and importantly the relationship between stacking of dibenzofuran groups and the multiple emission centers in dibenzofuran-containing compounds was explored by virtue of X-ray single crystal diffraction and theoretical calculations. Due to the tri-emission centers in 3-SPhF, color-tunable luminescence was achieved in both delay and steady states. On the one hand, the proportion of monomeric phosphorescence (τ = 497.7 ms) and aggregated-state phosphorescence (τ = 230.0 ms) was adjusted to render time-dependent afterglow. Besides, the excitation-dependent emission was realized in a steady state through controlling the conventional fluorescence and delayed fluorescence (τ = 282.5 μs). Meanwhile, the different colors between the illuminated side and shadow side were observed due to the attenuation of excitation. The successful exploration of multiple emission centers in compounds with a dibenzofuran group will pave the way for the development of color-tunable luminescent materials.

Data availability

All the data supporting this article have been included in the main text and the supplementary information.

Author contributions

J. R. synthesized compounds and measured photophysical properties. X. C. and Y. L. performed theoretical calculations. Y. L. measured X-ray single crystal diffraction. J. R. wrote the

manuscript. J. Z. revised the manuscript. All the authors contributed to the discussion of results.

Conflicts of interest

There are no conflicts to declare.

Acknowledgements

Notes and references

1 Q. Dai and A. Nelson, *Chem. Soc. Rev.*, 2021, **39**, 4057–4066.
2 Z. Chi, X. Zhang, B. Xu, X. Zhou, C. Ma, Y. Zhang, S. Liu and J. Xu, *Chem. Soc. Rev.*, 2021, **41**, 3878–3896.
3 K. Li, Y. Xiang, X. Wang, J. Li, R. Hu, A. Tong and B. Z. Tang, *J. Am. Chem. Soc.*, 2014, **136**, 1643–1649.
4 S. Nowag and R. Haag, *Angew. Chem., Int. Ed.*, 2014, **53**, 49–51.
5 J. P. Magnusson, A. Khan, G. Pasparakis, A. O. Saeed, W. Wang and C. Alexander, *J. Am. Chem. Soc.*, 2008, **130**, 10852–10853.
6 M. G. Cowan, J. Olguín, S. Narayanaswamy, J. L. Tallon and S. Brooker, *J. Am. Chem. Soc.*, 2012, **134**, 2892–2894.
7 J. Hu, G. Zhang and S. Liu, *Chem. Soc. Rev.*, 2012, **41**, 5933–5949.
8 D. B. Papkovsky and R. I. Dmitriev, *Chem. Soc. Rev.*, 2013, **42**, 8700–8732.
9 G. M. Farinola and R. Ragni, *Chem. Soc. Rev.*, 2011, **40**, 3467–3482.
10 M. Irie, T. Fukaminato, K. Matsuda and S. Kobatake, *Chem. Rev.*, 2014, **114**, 12174–12277.
11 Y. Zhou, W. Qin, C. Du, H. Gao, F. Zhu and G. Liang, *Angew. Chem., Int. Ed.*, 2019, **58**, 12102–12106.
12 W. Xu, Y. Yu, X. Ji, H. Zhao, J. Chen, Y. Fu, H. Cao, Q. He and J. Cheng, *Angew. Chem., Int. Ed.*, 2019, **58**, 16018–16022.
13 J. Wei, X. Jiao, T. Wang and D. Chen, *ACS Appl. Mater. Interfaces*, 2016, **8**, 29713–29720.
14 M. Natali and S. Giordani, *Chem. Soc. Rev.*, 2012, **41**, 4010–4029.
15 Z. Mao, Z. Yang, Y. Mu, Y. Zhang, Y. Wang, Z. Chi, C. Lo, S. Liu, A. Lien and J. Xu, *Angew. Chem., Int. Ed.*, 2015, **54**, 1–5.
16 J. Chen, H. Tian, Z. Yang, J. Zhao, Z. Yang, Y. Zhang, M. P. Aldred and Z. Chi, *Adv. Opt. Mater.*, 2021, **9**, 2001550.
17 L. Bian, H. Ma, W. Ye, A. Lv, H. Wang, W. Jia, L. Gu, H. Shi, Z. An and W. Huang, *Sci. China: Chem.*, 2020, **63**, 1443–1448.
18 J. Wang, Y. Fang, C. Li, L. Niu, W. Fang, G. Cui and Q. Yang, *Angew. Chem., Int. Ed.*, 2020, **59**, 10032–10036.
19 Z. Yang, E. Ubba, Q. Huang, Z. Mao, W. Li, J. Chen, J. Zhao, Y. Zhang and Z. Chi, *J. Mater. Chem. C*, 2020, **8**, 7384–7392.
20 S. Behera, S. Park and J. Gierschner, *Angew. Chem., Int. Ed.*, DOI: 10.1002/anie.202009789.
21 N. A. Kukhta and M. R. Bryce, *Mater. Horiz.*, 2021, **8**, 33–55.
22 J. Chen, T. Yu, E. Ubba, Z. Xie, Z. Yang, Y. Zhang, S. Liu, J. Xu, M. P. Aldred and Z. Chi, *Adv. Opt. Mater.*, 2019, **7**, 1801593.
23 G. Yue, X. She, J. Ma and X. Pan, *Chin. J. Appl. Chem.*, 2004, **21**, 20–23.
24 S. Hirata, H. Hara and I. Bhattacharjee, *J. Phys. Chem. C*, 2020, **124**, 25121–25132.
25 Z. Yang, Z. Mao, X. Zhang, D. Ou, Y. Mu, Y. Zhang, C. Zhao, S. Liu, Z. Chi, J. Xu, Y. Wu, P. Lu, A. Lien and M. R. Bryce, *Angew. Chem., Int. Ed.*, 2016, **55**, 2181–2185.
26 W. Zhao, Z. He, J. W. Y. Lam, Q. Peng, H. Ma, Z. Shuai, G. Bai, J. Hao and B. Z. Tang, *Chem*, 2016, **1**, 592–602.
27 S. Kuno, H. Akeno, H. Ohtani and H. Yuasa, *Phys. Chem. Chem. Phys.*, 2015, **17**, 15989–15995.
28 S. Hirata, *Adv. Opt. Mater.*, 2017, **5**, 1700116.
29 T. Lu and F. Chen, *J. Comput. Chem.*, 2012, **33**, 580–592.